Environmental Research 216 (2023) 114594

Contents lists available at ScienceDirect

Environmental Research

journal homepage: www.elsevier.com/locate/envres

Cobalt nanoparticles synthesizing potential of orange peel aqueous extract and their antimicrobial and antioxidant activity

Wongchai Anupong [a,d,*], Ruangwong On-uma [b,d], Kumchai Jutamas [c,d], Deepika Joshi [e], Saleh H. Salmen [f], Tahani Awad Alahmadi [g], G.K. Jhanani [h]

[a] Department of Agricultural Economy and Development, Faculty of Agriculture, Chiang Mai University, 50200, Thailand
[b] Department of Entomology and Plant Pathology, Faculty of Agriculture, Chiang Mai University, 50200, Thailand
[c] Department of Plant Science and Soil Sciences, Faculty of Agriculture, Chiang Mai University, Chiang Mai, 50200, Thailand
[d] Innovative Agriculture Research Center, Faculty of Agriculture, Chiang Mai University, Chiang Mai, 50200, Thailand
[e] Department of Oral Biology, University of Louisville, Kentucky, USA
[f] Department of Botany and Microbiology, College of Science, King Saud University, PO Box -2455, Riyadh, 11451, Saudi Arabia
[g] Department of Pediatrics, College of Medicine and King Khalid University Hospital, King Saud University, Medical City, PO Box-2925, Riyadh, 11461, Saudi Arabia
[h] Center for Transdisciplinary Research (CFTR), Department of Pharmacology, Saveetha Dental College, Saveetha Institute of Medical and Technical Sciences, Saveetha University, Chennai, India

ARTICLE INFO

Keywords:
Orange peel
Cobalt nanoparticles
Characterization
Antimicrobial
Antioxidant

ABSTRACT

The ability of cobalt nanoparticles (CoNPs) to absorb electromagnetic waves led to their use as potential biomedical agents in recent years. The properties of magnetic fluid containing cobalt nanoparticles are extraordinary. Hence, this research was designed to evaluate the $Co(NO_3)_2$ reducing the potential of orange peel aqueous extract and assessed their antimicrobial and antioxidant activities. The aqueous extract derived from orange peel had the potential to fabricate the CoNPs from 1 M $Co(NO_3)_2$ and the synthesized CoNPs were successfully characterized by standard nanoparticles characterization techniques such as UV–vis spectrophotometer, Fourier Transform Infrared Spectroscopy (FTIR), Scanning Electron Microscope (SEM), and Dynamic light scattering (DLS) analyses. The FTIR analysis revealed that the synthesized CoNPs were capped with active functional groups. It was characterized by predominant peaks corresponding to carbonyl (C═O), amide (CO =), and C–O of alcohols or phenols. The size and shape of CoNPs were found as 14.2–22.7 nm and octahedral, respectively, under SEM analysis. Furthermore, at increased concentration, the CoNPs demonstrated remarkable antimicrobial activity against common bacterial (*Escherichia coli*, *Staphylococcus aureus, Bacillus subtilis*, and *Klebsiella pneumoniae*) and fungal (*Aspergillus niger*) pathogens. Furthermore, these CoNPs also showed considerable *in-vitro* antioxidant activities against various free articles such as 2,2-diphenyl-1-picrylhydrazyl (DPPH), and Hydrogen Peroxide (H_2O_2). These results suggest that OP aqueous extract synthesized CoNPs possess considerable biomedical applications.

1. Introduction

The citrus fruits (orange) are one of the most popular fruits worldwide. The tangy flavor of fresh oranges has numerous health benefits. This wonder fruit is beneficial to the skin, losing weight, as well as the immune response (Sharmila et al., 2020). Though we all understand, oranges are a good source of Vitamin C and some other vital phytonutrients (Williams, 2013). Meanwhile, the orange peel, which we usually discard, contains nutrients such as fiber, folate, calcium, vitamin B6, vitamin C, and many others. Furthermore, the orange peel contains a high concentration of polyphenols, which protect against various diseases (Sharmila et al., 2020). Because of the existence of limonene, a naturally present compound, it also possesses fine anti-cancerous attributes. Besides that, the essential oil extracted from the orange peel has anti-inflammatory characteristics which boost our immune system (de la Torre et al., 2019). Orange peel, the major waste portion in the manufacturing of orange juice, contains flavonoids (fractions such as *O*-glycosylated flavanones, *O*-glycosylated flavonols, polymethoxylated flavones, phenolic acids, *O*-glycosylated flavones, and *C*-glycosylated flavones) and their ester derivatives possess considerable antioxidant

* Corresponding author. Department of Agricultural Economy and Development, Faculty of Agriculture, Chiang Mai University, Chiang Mai, 50200, Thailand.
E-mail addresses: anupong.w@cmu.ac.th (W. Anupong), jhanani15k@gmail.com (G.K. Jhanani).

https://doi.org/10.1016/j.envres.2022.114594
Received 18 August 2022; Received in revised form 26 September 2022; Accepted 12 October 2022
Available online 17 October 2022

(DPPH) properties (Kanaze et al., 2009). The orange peel extracts' presumed antioxidant potential is primarily attributed to the glycosides hesperidin and naringin (Williams, 2013). Coniferin and phlorin are two more phenolic compounds present in orange peels, which have been shown to help with radical scavenging while taken in the portion of orange peel molasses (Negro et al., 2017). These phytochemicals enriched orange peel has been used in this study as a novel approach to synthesize the CoNPs from cobalt sulfate heptahydrate. Since nanoparticles have gained investigators from various fields over the last few decades due to their elevated surface-to-volume ratio and other truly unique characteristics (Samuel et al., 2020; Narayanan et al., 2022). Among various nanoparticles, the cobalt and cobalt oxide nanoparticles have a wide range of biomedical applications such as antioxidant, antimicrobial, anticancer, insecticidal, antiparasitic, antidepressant, wound healing, as well as antidiabetic activities (Rajeswari et al., 2021; Waris et al., 2021). Apart from various biomedical applications, the cobalt and cobalt oxide nanoparticles have been extensively used in rechargeable (lithium-ion) batteries, colorants, thin electronic layers, resistors, gas sensing, photocatalysis, and as pollutant remediation (Medvedeva et al., 2017; Waris et al., 2021). Various chemical and physical methods are being used; notwithstanding, such methods may be affiliated with eco-toxicity, expense, high energy, and time consumption (Waris et al., 2021). Thus, the researchers prefer to use biological materials to synthesize the nanoparticles since it is eco-friendly, cost-effective, and less time-consuming. Furthermore, the chemicals from the biomaterials may directly involve the reduction or synthesis of nanoparticles and interestingly coated over the surface of synthesized particles (Okwunodulu et al., 2019). Hence, the phytochemicals enriched aqueous extract of orange peel was used to synthesize and characterize (UV–vis- spectrophotometer, Fourier-transform infrared spectroscopy (FTIR), Dynamic Light Scattering (DLS), and Scanning Electron Microscope (SEM)) the cobalt nanoparticle (CoNPs) from $CoSO_4{\cdot}7H_2O$. Furthermore, the possible *in-vitro* biomedical applications such as antimicrobial (Bacteria: *Staphylococcus aureus, Bacillus subtilis, Escherichia coli,* and *Klebsiella pneumoniae.* Fungi: *Aspergillus niger*) and antioxidant (2,2-diphenyl-1-picrylhydrazyl (DPPH, Hydroxyl, H_2O_2, and Ferric Reducing Antioxidant Power Assay) activity potential of synthesized CoNPs were evaluated.

2. Materials and methods

2.1. Collection and processing of orange peel

The Orange Peel (OP) (*Citrus reticulata*) was collected from the regional market, and they were washed with sterile water and sliced into fine pieces. About 50 g of the fresh fine OP was used for aqueous extract preparation by blending with 200 mL of sterile deionized water and homogenized using an electric mixer (Premier-Turbo, EM-H50N–W). The homogenized mixer was then heated at 70 °C for 30 min, cooled at room temperature, and filtered through Whatman No.1 filter paper (Negro et al., 2017; Waris et al., 2021). This filtrate was then used to fabricate cobalt nanoparticles (CoNPs).

2.2. Synthesis of CoNPs

About 90 mL of freshly prepared OP aqueous extract was blended with 10 mL of freshly prepared Co $(NO_3)_2$ (1 M). This reaction mixture was heated for 90 min at 60 °C till reduced volume up to 30 mL and then kept undisturbed at room temperature overnight (Waris et al., 2021). After overnight incubation, the reaction mix was centrifuged for 15 min 10,000 rpm. The obtained pellet was rinsed with deionized water and ethanol to remove un-reacted particles and impurities. The obtained precipitates were dried in an oven at 65 °C for 8–9 h, grinded, and subjected to characterization (Bibi et al., 2017).

2.3. Characterization of OP synthesized CoNPs

2.3.1. UV–visible spectrophotometer analysis

The standard protocol (Kharade Suvarta et al., 2020) was followed to confirm the reduction of 1 M $Co(NO_3)_2$ into CoNPs mediated by OP aqueous extract was studied by reading the absorbance of 1 mL of CoNPs at 200–800 nm through UV–vis. Spectrophotometer (V-760 UV–Visible Spectrophotometer, Jasco, Pvt. Ltd.).

2.4. FTIR analysis

The functional groups of bioactive components of OP aqueous extract, which involved in the reduction of $Co(NO_3)_2$ into CoNPs as well as a coat over the surface of them was identified through Fourier Transform Infrared Spectroscopy (iS5 FTIR Spectrometer, Thermo Scientific Nicolet) in the range of 400–4000 cm^{-1} with a resolution of 8 cm^{-1} in the presence of KBr pellets by following standard operating protocol (Hafeez et al., 2020).

2.4.1. SEM and DLS analysis

The size and structural morphology of OP aqueous extract synthesized CoNPs were examined through Scanning Electron Microscope (JSM-7900 F Schottky Field Emission SEM-JEOL, Ltd) under the magnifications of magnification of 5.00 KX to 15.00 KX with the standard operating protocol. The size distribution pattern and the average size of OP aqueous extract of synthesized CoNPs were studied through Dynamic light scattering analysis (MADLS-Zetasizer Ultra, Malvern Panalytical Ltd.).

2.5. Antimicrobial activity potential of CoNPs

The antimicrobial activity of OP aqueous extract synthesized CoNPs was studied by standard agar well diffusion method with Mueller Hinton Agar (MHA) media against common bacterial (*Escherichia coli*, *Staphylococcus a*ureus, *Bacillus subtilis*, and *Klebsiella pneumoniae*) and fungal pathogens (*Aspergillus niger*). In brief, the test microbial pathogens were inoculated on sterilized MHA-containing plates through the spread plate method. Then various concentrations (50, 100, and 150 μg mL^{-1}) of OP aqueous extract synthesized CoNPs were poured on well-perforated plates in triplicates. About 75 μg mL^{-1} (each) concentration of tetracycline and fluconazole were used as a positive control for bacteria and fungus respectively. The inoculated plates (triplicates) along with sterile and positive control plates were incubated at 35 °C and 28 °C for 24 h (for bacteria) and 72 h (fungus) of incubation, respectively. The size of the zone of inhibition (in mm) of various concentrations of CoNPs was measured and compared with positive control.

2.6. In-vitro free radicals scavenging potential of CoNPs

The free radicals scavenging competence of OP aqueous extract synthesized CoNPs was studied through standard *in-vitro* antioxidant assay against various forms of free radicals such as 2,2-diphenyl-1-picrylhydrazyl (DPPH), Hydroxyl (OH^-), Hydrogen Peroxide (H_2O_2), and Ferric Reducing Antioxidant Power (FRAP) assays.

2.6.1. DPPH assay

The DPPH free radicals scavenging competence of various dosages of OP aqueous extract synthesized CoNPs was studied following the typical method. In brief, about 2.0 mL of different concentration (200, 400, 600, 800, and 1000 μg mL^{-1}) of CoNPs were blend with 2.0 mL of DPPH (0.004%) solution. Furthermore, similar butylated hydroxytoluene (BHT) concentration was used as standard. These reaction mixtures were then incubated for 30 min under dark conditions. Each sample's absorption rate was read at 517 nm using a UV–vis spectrophotometer, and the percentage of DPPH free radicals scavenging activity was calculated using the following standard formula (Ajarem et al., 2022).

DPPH free radical scavenging activity (%) = (Control − Test/Control) × 100 [1]

2.6.2. Hydroxyl radicals scavenging activity

The ability of aqueous extract of OP synthesized CoNPs to scavenge hydroxyl (OH^-) radicals were tested using a standard protocol. Concisely, 0.45 mL of sodium phosphate (200 mM) buffer (pH-7.0), 0.15 mL of 10 mM deoxyribose, 0.150 mL of 10 mM FeSO4–EDTA, 0.15 mL of 10 mM H_2O_2, and 0.525 mL distilled water were blended with 0.075 mL of different concentrations (200–1000 μg mL^{-1}) of CoNPs. Each concentration of reaction mixture was incubated for 4 h. Later, 0.75 mL (each) of 2.8% Trichloroacetic Acid (TCA) and 1% Trichloroacetic Acid (TBA) supplementation inhibited the reaction. The reaction mixers were then placed in a boiling water bath for 10 min before cooling with tap water. The solution's absorbance was measured at 520 nm, and a similar concentration of BHT was used as standard.

Hydroxyl free radical scavenging activity (%) = (Control − Test/Control) × 100 [2]

2.6.3. H_2O_2 scavenging assay

The H_2O_2 scavenging activity of OP aqueous extract synthesized CoNPs was investigated using a standard protocol. In brief, 0.4 mL of different concentrations (200–1000 μg mL^{-1}) of CoNPs were mixed with 0.4 mL of H_2O_2 to make a total volume of 3.0 mL. After incubating the reaction mixer for 10 min, the absorbance at 230 nm was observed with a spectrophotometer. Similar concentrations of BHT were used as a control, and the percentage of H_2O_2 scavenging activity was calculated using the formula below (Kamal et al., 2020).

H2O2 free radical scavenging activity (%) = (Control − Test/Control) × 100 [3]

2.6.4. FRAP assay

The ferric reducing potential of OP synthesized CoNPs was evaluated by standard FRAP assay protocol using colorless or light brownish 2,4,6-tripyridyl-s-triazine (TPTZ) and ferric chloride hexahydrate complexes. In brief, 3 μL of different concentrations (each) of OP aqueous extract synthesized CoNPs were blended with 150 μL of complex ferric reagent in a cuvette and incubated for 10 min. After 10 min of incubation was, the color change was noticed (blue color formation indicates the reduction of ferrous complexes), and absorbance was then measured at 605 nm using UV–vis. Spectrophotometer and BHT were used as standard. The ferric complex, reducing percentage was calculated by following the standard formula.

FRAP activity (%) = (Control − Test/Control) × 100 [4]

3. Results and discussion

The results obtained in this study revealed that the aqueous extract of OP could fabricate/reduce the 1 M $Co(NO_3)_2$ into CoNPs. A UV–vis spectrophotometer confirmed the initial reduction of $Co(NO_3)_2$. The spectrophotometer analysis result showed the reduced form of $Co(NO_3)_2$ as CoNPs by founding the absorbance peak at 436 nm (Fig. 1). This wide surface Plasmon resonance (SPR) band indicates poly-dispersed nanomaterials. This fabrication was possible due to various phenolic compounds in the aqueous extract of OP. This result was correlated with the findings of Varaprasad et al. (2017). They reported that the absorbance of CoNPs synthesized by root extract of *Asparagus racemosus* was reported as narrow as well as smooth absorption at 438 nm (Varaprasad et al., 2017). Another study found that the absorbance of *Hibiscus cannabinus* leaf extract synthesized CoNPs was 508 nm (Kharade Suvarta et al., 2020).

The SPR band near 436 nm widened and shifted slightly towards the lengthy wavelength range, suggesting the existence and emergence of CoNPs (Padalkar et al., 2017). SPR dominates the optical absorption spectra of metallic nanoparticles that also shifts to higher wavelength as particle diameter increases (Solati et al., 2013). The position and structure of Co nanocluster plasmon absorption are greatly influenced by particle diameter, dielectric material, and surface-adsorbed species (Zhang et al., 2017). The SPR absorption of CoNPs with a short wavelength range in the visible range around 436 nm is caused by the same transverse electronic fluctuation (Varaprasad et al., 2017).

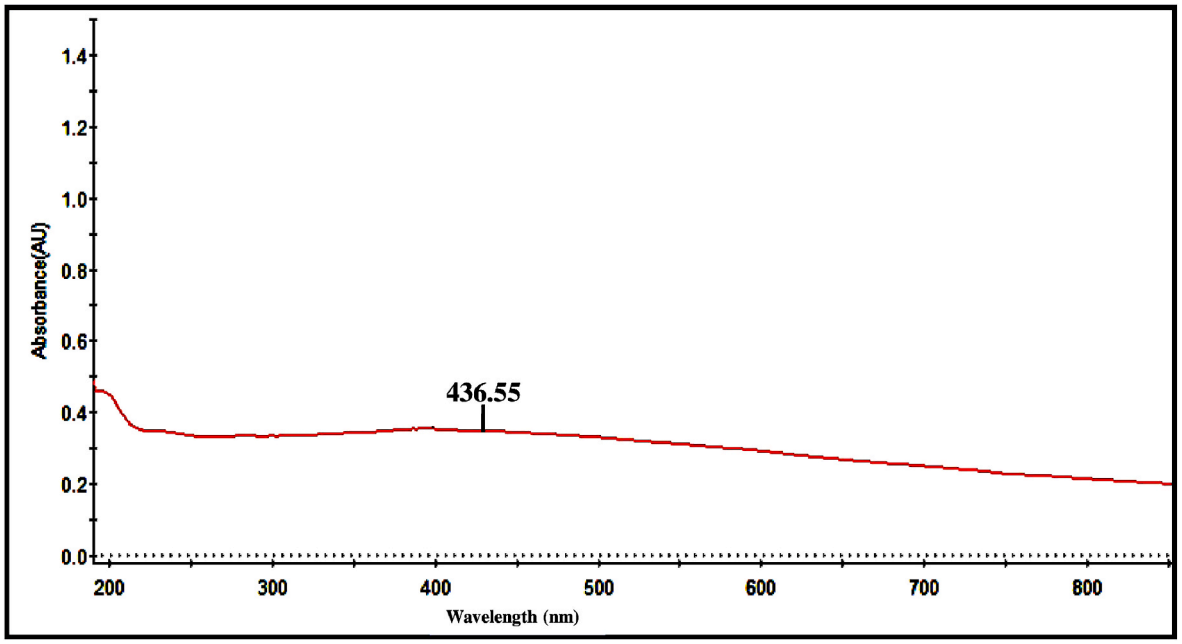

Fig. 1. UV–vis spectrophotometer analysis of orange peel mediated CoNPs.

3.1. FTIR characterization of CoNPs

The functional groups of phytochemicals of OP aqueous extract, which is responsible for the reduction of $Co(NO_3)_2$ and coated over the surface of the CoNPs as capping and act as a stabilizing, were analyzed FTIR. Few predominant peaks were found at 3423.74, 2922.72, 2852.36, 1629.77, 1317.35, 1113.51, 663.32, 648.31, 576.86, and 530.15 cm^{-1} (Fig. 2). The peak found at 3423.74 cm^{-1} attributed to the hydroxyl group of various phenolic components. The peaks found at 2922.72 and 2852.36 cm^{-1} correspond to C– asymmetric stretching vibrations. Some other major peaks found at 1629.77, 1317.35, 1113.51, and 530.15 cm^{-1} corresponded to carbonyl (C═O), amide (CO =), C–O of alcohols or phenols, as well as CoNPs, respectively (Fig. 2). These results strongly suggest that the OP aqueous extract contains more phenolic and other reducing phytochemical components. These results were correlated with the findings of *Populus ciliate* leaf extract synthesized CoNPs possess predominant peaks at 3458, 1622, 1381, 1082, and 533 cm^{-1} (Hafeez et al., 2020). Similarly, Varaprasad et al. (2017) reported that significant predominant peaks (3442.90 cm^{-1} = OH & C═O, 1597 cm^{-1} – COOH, 1357 cm^{-1} = C–O) corresponding various forms of phenolics and other compounds, which involved in the reduction and capping of CoNPs synthesized by aqueous extract of *Asparagus racemosus* (Varaprasad et al., 2017). Another report was correlated with the present findings: the FTIR peaks obtained at 3293 cm^{-1} (-OH groups), 1634 cm^{-1} (C═O of –COOH groups), 1350 cm^{-1} (C–O) CoNPs synthesized and capped by *Hibiscus cannabinus* leaf extract (Kharade Suvarta et al., 2020).

3.2. DLS and SEM analyses

The hydrodynamic dimensions of OP aqueous extract synthesized CoNPs were analyzed through DLS analysis. The results obtained from the DLS analysis demonstrated that uniform size scattering/distribution of OP synthesized CoNPs with the average hydrodynamic size as 132 nm (Fig. 3). Similarly, the SEM analysis results revealed that the size of OP aqueous extract synthesized CoNPs was ranged from 14.2 to 22.7 nm with different magnifications and octahedral-shaped nanoparticles. The author's knowledge may be the first report about OP aqueous extract synthesized octahedral-shaped CoNPs (Fig. 4). This result was correlated with the findings of Akhlaghi et al. (2020). They reported that the size and shape of CoNPs synthesized by *Trigonella foenumgraceum* ethanol

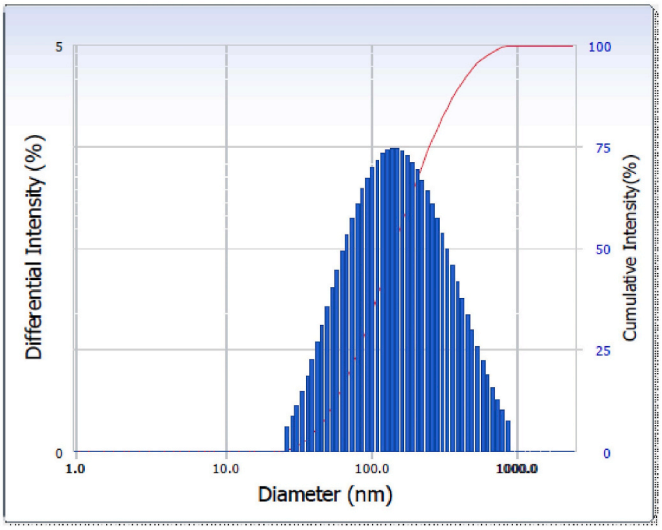

Fig. 3. Intensity distribution pattern of orange peel mediated CoNPs analyzed by Dynamic Light Scattering (DLS).

extract were 13.2 nm and quasi-spherical, respectively (Akhlaghi et al., 2020). The size and shape obtained from this study can be used in various biomedical and non-medical applications (Shah et al., 2012). The size and shape of CoNPs are determined by the quality and quantity of bioactive components present in the aqueous extract of OP (Sudagar et al., 2021). Furthermore, the reaction time and phytochemicals involved in the capping and reduction potential also determine the size and shape of the nanoparticles (Akhlaghi et al., 2020).

3.3. Antimicrobial activity potential analysis

The antimicrobial potential of OP aqueous extract synthesized CoNPs against some common microbial pathogens such as *E. coli, S. aureus, B. subtilis, K. pneumoniae,* and *A. niger* through the agar well diffusion method. The obtained results revealed that the synthesized CoNPs showed dose-dependent antimicrobial activity against test microbial pathogens. The increased significant antibacterial activity was found against test bacterial pathogens in the order of *E. coli* (24 ± 1.3) > *K. pneumoniae* (22 ± 1.5) > *B. subtilis* (21 ± 1.6) > *S. aureus* (18 ± 1.5) at

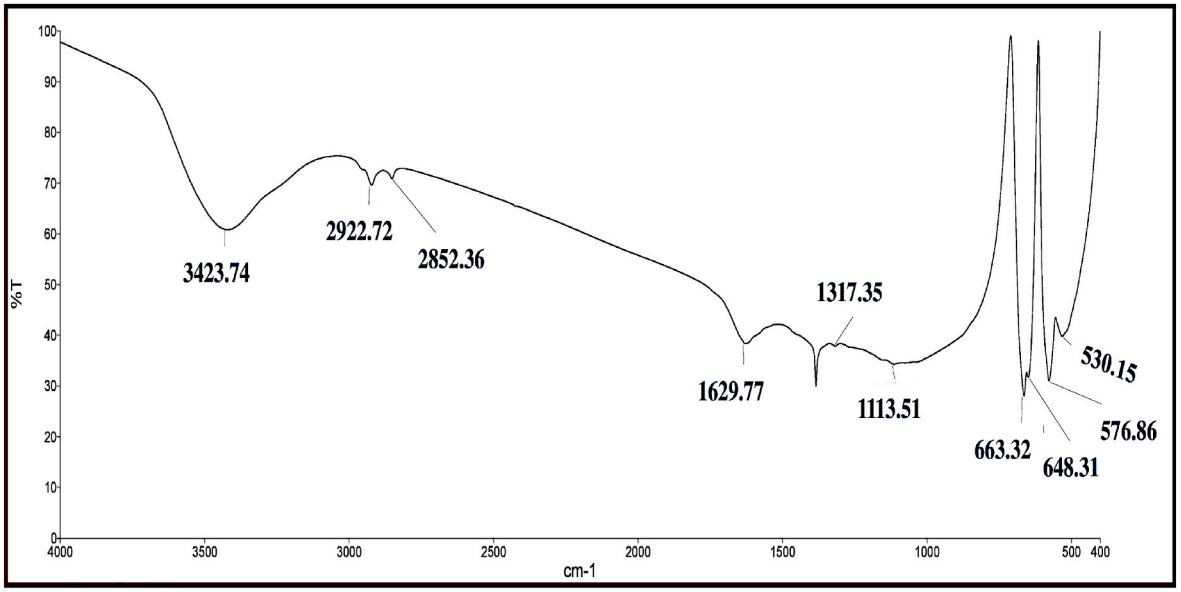

Fig. 2. FTIR spectrum of orange peel mediated CoNPs.

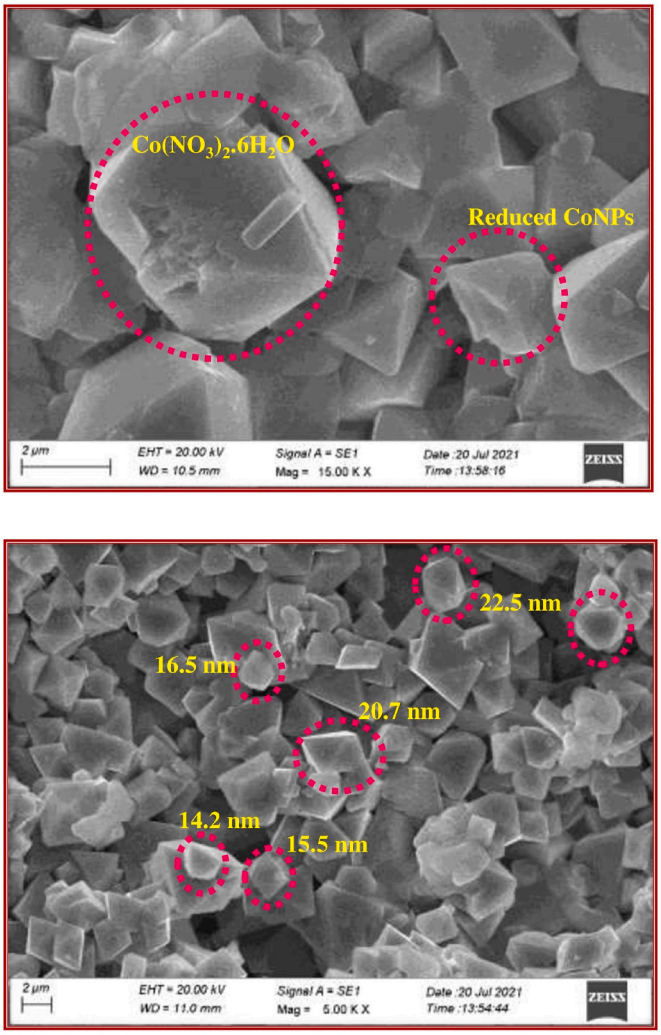

Fig. 4. The size and morphological traits of orange peel mediated CoNPs by SEM analysis.

200 μg mL^{-1} concentrations of CoNPs (Table 1). Interestingly, the obtained zone of inhibition was greater than the zone of inhibition of 75 μg mL^{-1} concentration of tetracycline (positive control). Similarly, an increased concentration (200 μg mL^{-1}) of CoNPs showed effective antifungal activity against *A. niger,* and it was greater than the zone of inhibition of 75 μg mL^{-1} concentration of Fluconazole (Table 1). These antimicrobial properties of OP aqueous extract synthesized CoNPs might be due to the bioactive compounds involved in the reduction and capping over the surface of the CoNPs (Zhao et al., 2021). Similarly, the *Populus ciliata* leaf extract mediated CoNPs showed considerable antibacterial activity (14.0 ± 0.6 to 21.8 ± 0.7) in dose-dependent manner against *E. coli, B. lichenifermia, K. pneumoniae,* and *B. subtillus* (Hafeez et al., 2020). Another report stated that the *Celosia argentea* mediated CoNPs possess remarkable antimicrobial activity against *E. coli* and *B. subtilus* as 51.83 mm and 42.18 mm respectively (Shahzadi et al., 2019). The CoNPs fabricated from Aerva javanica extract possess significant antibacterial (*B. subtilis*, *S. aureus*, *E. coli*, and *P. aeruginosa*) and antifungal activity (*Fusarium solani*) at a concentration of 3.13 mg mL^{-1} (Mubraiz et al., 2021).

Table 1
Antimicrobial activity potential of orange peel aqueous extract mediated CoNPs.

Name of microbial pathogens	Various concentrations (μg mL^{-1}) of CoNPs			
	50	100	200	Positive control (Tetracycline: 75 μg mL^{-1})
E. coli	17 ± 1.7	19 ± 2.1	24 ± 1.3	18 ± 1.4
S. aureus	16 ± 1.5	17 ± 1.4	18 ± 1.5	17 ± 1.5
B. subtilis	17 ± 1.1	18 ± 1.3	21 ± 1.6	18 ± 1.9
K. pneumoniae	19 ± 1.8	18 ± 1.6	22 ± 1.5	19 ± 1.3
A. niger	18 ± 1.6	19 ± 1.8	21 ± 1.4	19 ± 1.7 (Fluconazole: 75 μg mL^{-1})

Legend: Mentioned values are mean and standard error (±SE) of triplicates.

3.4. Free radicals scavenging potential

3.4.1. DPPH scavenging assay

The free radicals scavenging competence of OP aqueous extract synthesized CoNPs was studied against the DPPH radicals through standard assay. The results obtained from this study revealed that the synthesized CoNPs effectively scavenged the 2,2-diphenyl-1-picrylhydrazyl (DPPH) into 2,2-diphenyl-1-picrylhydrazine (DPPH-H) and altered the color as pale-yellowish. These color changes were monitored through spectrophotometer analysis. The dose-dependent antioxidant activity was 62.17% at 1000 μg mL^{-1} concentration, and however, it was considerably lower than the DPPH radicals scavenging activity of positive control (Fig. 5a and b). The phenolic components that capped the CoNPs possess might be responsible for their antioxidant potential by donating the H^+ and binding with free radicals to scavenge them (Rehana et al., 2017). The *Sageretia thea* aqueous leaf extract synthesized CoNPs possess considerable DPPH free radicals scavenging activity (Khalil et al., 2020). Similarly, the *Hibiscus rosasinensis* aqueous leaf extract synthesized CoNPs was reported to have remarkable antioxidant activity against various forms of free radicals (Kainat et al., 2021). Interestingly, another report suggested that the leaf extract

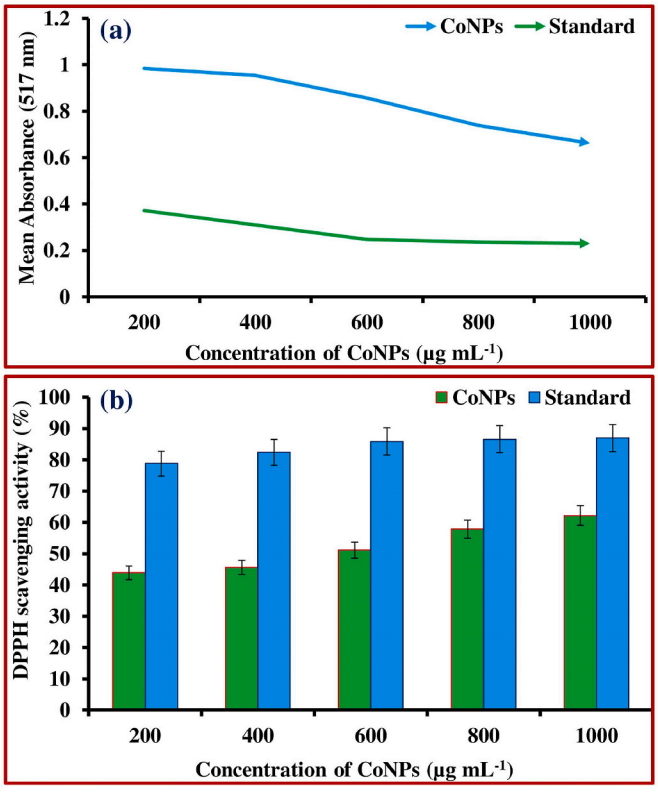

Fig. 5. DPPH free radicals scavenging activity of CoNPs. (a) Mean absorbance of CoNPs (b) DPPH scavenging activity (%).

Cadiospermum halicacebium synthesized CoNPs could scavenge different forms of free radicals (Malathy and Revathi, 2021).

3.4.2. Hydroxyl scavenging assay

The OP aqueous extract synthesized CoNPs showed considerable free radicals scavenging activity comparable with positive control. Furthermore, the obtained results revealed that the synthesized CoNPs possess dose-dependent hydroxyl (OH^-) radicals scavenging activity as 72.18% at 1000 μg mL^{-1} concentration, and it was partially comparable with the hydroxyl radical scavenging potential of similar concentration of standard antioxidant agents (88.31%) (Fig. 6a and b). This scavenging potential was comparably significant for the partial pure for test nanoparticles. The flavonoids and other phenolic compounds that coat the surface of nanoparticles play an important role in hydroxyl radical scavenging (Sathishkumar et al., 2016).

A most responsive oxygen-centered species seems to be the OH^{-1} radical that also causes serious damage to surrounding biomolecules. The activity of OH radical scavenging was determined by producing hydroxyl radicals with ascorbic acid–iron EDTA (Pavithra and Vadivukkarasi, 2015). The fruit extract synthesized and carbon blended CoNPs were reported to possess remarkable hydroxyl radicals scavenging activity and increased concentration (Song et al., 2019).

3.4.3. H_2O_2 scavenging and FRAP assays

The aqueous extract of OP mediated CoNPs showed moderate H_2O_2 radicals scavenging activity, which was dose-dependent. Since at increased concentrations (1000 μg mL^{-1}), the CoNPs scavenged the H_2O_2 up to 55.78%, and this was comparatively lower than the H_2O_2 scavenging potential of standard (71.36%) (Fig. 7a and b). These results suggest that the bioactive compounds from OP extract involved in the capping and stabilizing activity on CoNPs synthesis possess the lowest H_2O_2 scavenging activity compared to other forms of free radicals. According to the authors' knowledge, this is the first report about the H_2O_2 scavenging potential of CoNPs synthesized from OP aqueous extract. Accordingly, the CoNPs synthesized through the electrochemical process showed considerable H_2O_2 radical scavenging activity (Kamal et al., 2020). There is no adequate report about the H_2O_2 radicals scavenging potential of CoNPs mediated through plant extracts. Some particular molecules (synthetic form) conjugated nanoparticles showed considerable H_2O_2 radicals scavenging activity. For example, the BSA blended (conjugated) MnO_2 nanoparticles demonstrated remarkable H_2O_2 scavenging activity (Pardhiya et al., 2020). The OP-mediated CoNPs effectively reduced the ferric (Fe^{+3}) into ferrous (Fe^{+2}) in the existence of TPTZ and formed strong blue Fe^{+2} – TPTZ complex color formation. At a concentration of 1000 μg mL^{-1}, the OP aqueous extract mediated CoNPs effectively reduced the ferric into ferrous up to 76.18%. It was almost comparable with the ferric reducing competence of the standard (84.32%) (Fig. 8a and b). It is the novel report about the ferric reducing potential of CoNPs synthesized by aqueous extract of OP as per the author's knowledge. The bioactive compounds capped on CoNPs can act as a hydrogen donor, breaking down the free radical chain and converting ferric to ferrous (Zhou et al., 2020). Under slightly acidic conditions, the phenolic acids, polyphenolics, flavonoids, and other compounds (Salari et al., 2019) found in plant extracts used in the capping and fabrication of CoNPs may effectively reduce ferric to ferrous (Veisi et al., 2021). Furthermore, the ferric reducing percentage was proportional to the quantity (Messaoud et al., 2012) and quality of ferric reducing phytochemicals, as well as the reaction time.

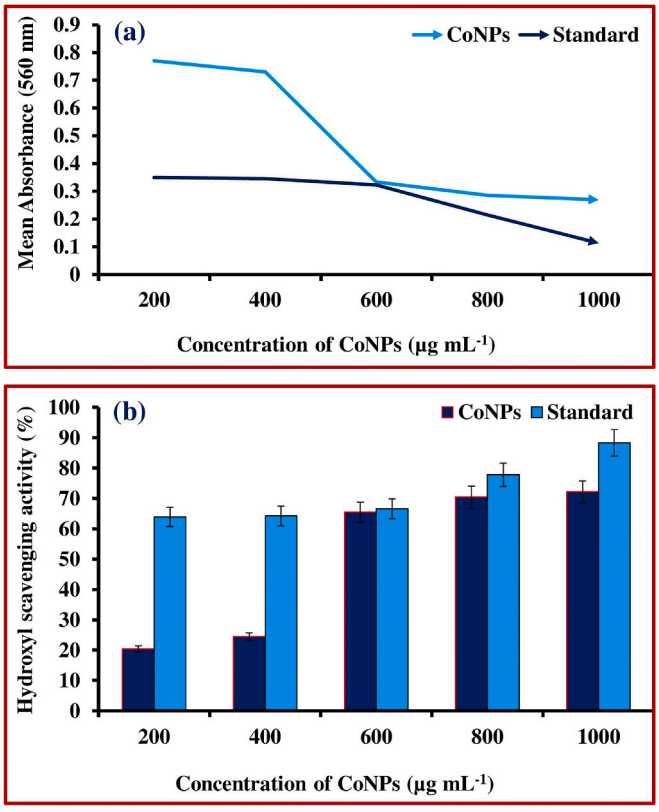

Fig. 6. Hydroxyl radicals scavenging activity of CoNPs. (a) Mean absorbance of CoNPs (b) Hydroxyl scavenging activity (%).

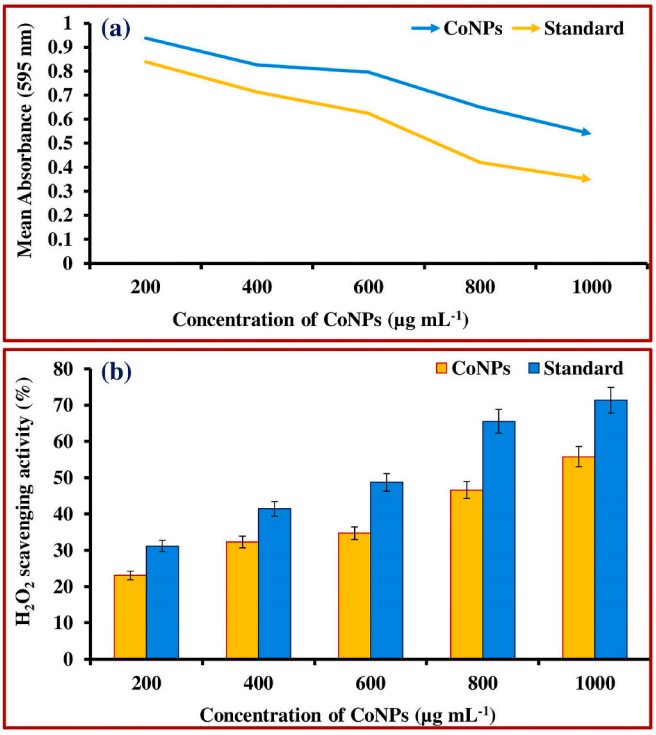

Fig. 7. H_2O_2 radicals scavenging activity of CoNPs. (a) Mean absorbance of CoNPs (b) H_2O_2 scavenging activity (%).

4. Conclusion

The phytochemicals in the aqueous extract of OP can effectively fabricate CoNPs from 1 M $Co(NO_3)_2$. The OP-mediated CoNPs were successfully characterized using UV–vis spectrophotometer, FTIR, DLS, and SEM analyses. Fortunately, at higher concentrations (200 μg mL^{-1}), the OP-mediated CoNPs have significant antimicrobial activity against *E. coli, S. aureus, B. subtilis, K. pneumoniae,* and *A. niger*. Surprisingly, these CoNPs have important *in-vitro* free radical scavenging activity

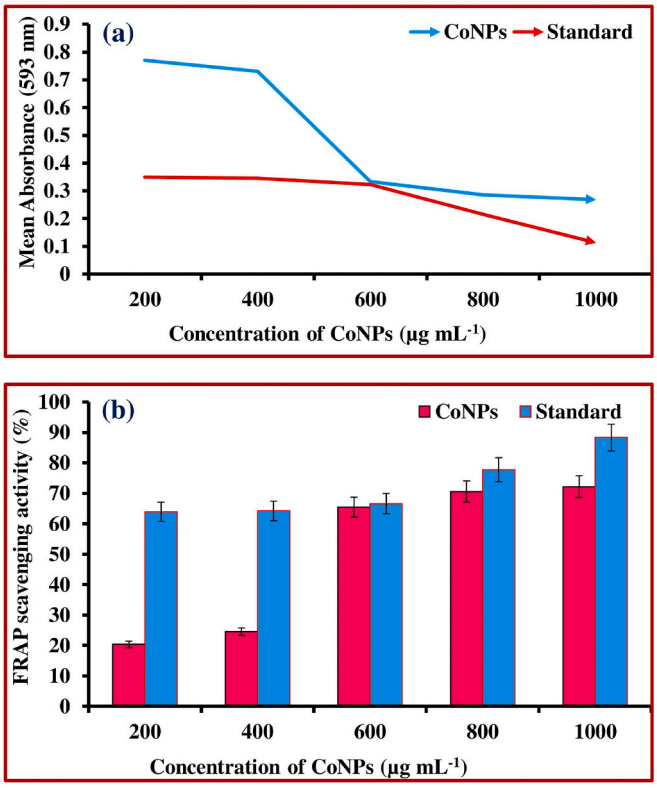

Fig. 8. FRAP of CoNPs. (a) Mean absorbance of CoNPs (b) DPPH scavenging activity (%).

against various free - radicals (DPPH, OH, H_2O_2, and Ferric compounds). These findings strongly suggest that the OP aqueous extract-mediated CoNPs may be significant for a wide range of biomedical applications after the *in-vivo* study results.

Credit author statement

Wongchai Anupong: Conceptualization, Writing- Original draft preparation, Supervision, Project administration. **Ruangwong Onuma:** Methodology, Writing- Original draft preparation, **Kumchai Jutamas:** Writing, Reviewing and Editing, **Deepika Joshi:** Writing, Reviewing and Editing, **Saleh H. Salmen:** Writing, Reviewing and Editing, **Tahani Awad Alahmadi:** Writing, Reviewing and Editing, **G.K. Jhanani:** Writing, Reviewing and Editing.

Declaration of competing interest

The authors declare that they have no known competing financial interests or personal relationships that could have appeared to influence the work reported in this paper.

Data availability

The data that has been used is confidential.

Acknowledgement

This research work was partially supported by Chiang Mai University. This project was supported by Researchers Supporting Project number (RSP-2021/385) King Saud University, Riyadh, Saudi Arabia.

References

Ajarem, J.S., Maodaa, S.N., Allam, A.A., Taher, M.M., Khalaf, M., 2022. Benign synthesis of cobalt oxide nanoparticles containing red algae extract: antioxidant, antimicrobial, anticancer, and anticoagulant activity. J. Cluster Sci. 33, 717–728. https://doi.org/10.1007/s10876-021-02004-9.

Akhlaghi, N., Najafpour-Darzi, G., Younesi, H., 2020. Facile and green synthesis of cobalt oxide nanoparticles using ethanolic extract of Trigonella foenumgraceum (Fenugreek) leaves. Adv. Powder Technol. 31, 3562–3569.

Bibi, I., Nazar, N., Iqbal, M., Kamal, S., Nawaz, H., Nouren, S., Safa, Y., Jilani, K., Sultan, M., Ata, S., Rehman, F., Abbas, M., 2017. Green and eco-friendly synthesis of cobalt-oxide nanoparticle: characterization and photo-catalytic activity. Adv. Powder Technol. 28, 2035–2043.

de la Torre, I., Martin-Dominguez, V., Acedos, M.G., Esteban, J., Santos, V.E., Ladero, M., 2019. Utilisation/upgrading of orange peel waste from a biological biorefinery perspective. Appl. Microbiol. Biotechnol. 103, 5975–5991.

Hafeez, M., Shaheen, R., Akram, B., Haq, S., Mahsud, S., Ali, S., Khan, R.T., 2020. Green synthesis of cobalt oxide nanoparticles for potential biological applications. Mater. Res. Express 7, 025019.

Kainat, Khan, M.A., Ali, F., Faisal, S., Rizwan, M., Hussain, Z., Zaman, N., Afsheen, Z., Uddin, M.N., Bibi, N., 2021. Exploring the therapeutic potential of Hibiscus rosa sinensis synthesized cobalt oxide (Co(3)O(4)-NPs) and magnesium oxide nanoparticles (MgO-NPs). Saudi J. Biol. Sci. 28, 5157–5167.

Kamal, N.M., Egzar, H.K., Ridha, N.A.-S., 2020. Electrochemical synthesis, characterization and evaluation of antioxidant activity of Co3 O4 nanoparticles and Co3 O4/TiO2 nanocomposite. EurAsia J. BioSci. 14, 3595–3600.

Kanaze, F.I., Termentzi, A., Gabrieli, C., Niopas, I., Georgarakis, M., Kokkalou, E., 2009. The phytochemical analysis and antioxidant activity assessment of orange peel (Citrus sinensis) cultivated in Greece–Crete indicates a new commercial source of hesperidin. Biomed. Chromatogr. 23, 239–249.

Khalil, A.T., Ovais, M., Ullah, I., Ali, M., Shinwari, Z.K., Maaza, M., 2020. Physical properties, biological applications and biocompatibility studies on biosynthesized single phase cobalt oxide (Co3O4) nanoparticles via Sageretia thea (Osbeck.). Arab. J. Chem. 13, 606–619.

Kharade Suvarta, D., Nikam Gurunath, H., Mane Gavade Shubhangi, J., Patil Sachinkumar, R., Gaikwad Kishor, V., 2020. Biogenic synthesis of cobalt nanoparticles using Hibiscus cannabinus leaf extract and their antibacterial activity. Res. J. Chem. Environ. 24, 9–13.

Malathy, D., Revathi, M., 2021. Green synthesis of cobalt nanoparticles using ethanolic extract of Cadiospermum halicacebium characterisation and its anti cancer applications. Cell 52, 9.

Medvedeva, O., Kambulova, S., Bondar, O., Gataulina, A., Ulakhovich, N., Gerasimov, A., Evtugyn, V., Gilmutdinov, I., Kutyreva, M., 2017. Magnetic cobalt and cobalt oxide nanoparticles in hyperbranched polyester polyol matrix. J. Nanotechnol. 2017.

Messaoud, C., Laabidi, A., Boussaid, M., 2012. Myrtus communis L. infusions: the effect of infusion time on phytochemical composition, antioxidant, and antimicrobial activities. J. Food Sci. 77, C941–C947.

Mubraiz, N., Bano, A., Mahmood, T., Khan, N., 2021. Microbial and plant assisted synthesis of cobalt oxide nanoparticles and their antimicrobial activities. Agronomy 11, 1607.

Narayanan, M., Priya, S., Natarajan, D., Alahmadi, T.A., Alharbi, S.A., Krishnan, R., Chi, N.T.L., Pugazhendhi, A., 2022. Phyto-fabrication of silver nanoparticle using leaf extracts of Aristolochia bracteolata Lam and their mosquito larvicidal potential. Process Biochem. 121, 163–169.

Negro, V., Ruggeri, B., Fino, D., Tonini, D., 2017. Life cycle assessment of orange peel waste management. Resour. Conserv. Recycl. 127, 148–158.

Okwunodulu, F.U., Chukwuemeka-Okorie, H.O., Okorie, F.C., 2019. Biological synthesis of cobalt nanoparticles from Mangifera indica leaf extract and application by detection of manganese (II) ions present in industrial wastewater. Chem. Sci. Int. J. 27, 1–8.

Padalkar, V.S., Tsutsui, Y., Sakurai, T., Sakamaki, D., Tohnai, N., Kato, K., Takata, M., Akutagawa, T., Sakai, K.-i., Seki, S., 2017. Optical and structural properties of ESIPT inspired HBT–fluorene molecular aggregates and liquid crystals. J. Phys. Chem. B 121, 10407–10416.

Pardhiya, S., Priyadarshini, E., Rajamani, P., 2020. In vitro antioxidant activity of synthesized BSA conjugated manganese dioxide nanoparticles. SN Appl. Sci. 2, 1597.

Pavithra, K., Vadivukkarasi, S., 2015. Evaluation of free radical scavenging activity of various extracts of leaves from Kedrostis foetidissima (Jacq.) Cogn. Food Sci. Hum. Wellness 4, 42–46.

Rajeswari, V.D., Khalifa, A.S., Elfasakhany, A., Badruddin, I.A., Kamangar, S., Brindhadevi, K., 2021. Green and ecofriendly synthesis of cobalt oxide nanoparticles using Phoenix dactylifera L: antimicrobial and photocatalytic activity. Appl. Nanosci. 1–9.

Rehana, D., Mahendiran, D., Kumar, R.S., Rahiman, A.K., 2017. Evaluation of antioxidant and anticancer activity of copper oxide nanoparticles synthesized using medicinally important plant extracts. Biomed. Pharmacother. 89, 1067–1077.

Salari, S., Esmaeilzadeh Bahabadi, S., Samzadeh-Kermani, A., Yosefzaei, F., 2019. In-vitro evaluation of antioxidant and antibacterial potential of green synthesized silver nanoparticles using prosopis farcta fruit extract. Iran. J. Pharm. Res. (IJPR) 18, 430–455.

Samuel, M.S., Selvarajan, E., Mathimani, T., Santhanam, N., Phuong, T.N., Brindhadevi, K., Pugazhendhi, A., 2020. Green synthesis of cobalt-oxide nanoparticle using jumbo Muscadine (Vitis rotundifolia): characterization and photo-catalytic activity of acid Blue-74. J. Photochem. Photobiol. B Biol. 211, 112011.

Sathishkumar, G., Jha, P.K., Vignesh, V., Rajkuberan, C., Jeyaraj, M., Selvakumar, M., Jha, R., Sivaramakrishnan, S., 2016. Cannonball fruit (Couroupita guianensis, Aubl.) extract mediated synthesis of gold nanoparticles and evaluation of its antioxidant activity. J. Mol. Liq. 215, 229–236.
Shah, S.A., Asdi, M.H., Hashmi, M.U., Umar, M.F., Awan, S.-U., 2012. Thermo-responsive copolymer coated MnFe2O4 magnetic nanoparticles for hyperthermia therapy and controlled drug delivery. Mater. Chem. Phys. 137, 365–371.
Shahzadi, T., Zaib, M., Riaz, T., Shehzadi, S., Abbasi, M.A., Shahid, M., 2019. Synthesis of eco-friendly cobalt nanoparticles using Celosia argentea plant extract and their efficacy studies as antioxidant, antibacterial, hemolytic and catalytical agent. Arabian J. Sci. Eng. 44, 6435–6444.
Sharmila, V.G., Kavitha, S., Obulisamy, P.K., Banu, J.R., 2020. Production of fine chemicals from food wastes. Food Waste Valuable Resour. 163–188. Elsevier.
Solati, E., Mashayekh, M., Dorranian, D., 2013. Effects of laser pulse wavelength and laser fluence on the characteristics of silver nanoparticle generated by laser ablation. Appl. Phys. A 112, 689–694.
Song, H., Li, X., He, Y., Peng, Y., Pan, J., Niu, X., 2019. Colorimetric Evaluation of the Hydroxyl Radical Scavenging Ability of Antioxidants Using Carbon-Confined CoO(x) as a Highly Active Peroxidase Mimic, vol. 186, p. 354.
Sudagar, A.J., Rangam, N.V., Ruszczak, A., Borowicz, P., Tóth, J., Kövér, L., Michałowska, D., Roszko, M., Noworyta, K.R., Lesiak, B., 2021. Valorization of brewery wastes for the synthesis of silver nanocomposites containing orthophosphate. Nanomaterials 11, 2659.
Varaprasad, T., Govindh, B., Rao, B., 2017. Green synthesized cobalt nanoparticles using Asparagus racemosus root extract & evaluation of antibacterial activity. Int. J. ChemTech Res. 10, 339–345.
Veisi, H., Karmakar, B., Tamoradi, T., Tayebee, R., Sajjadifar, S., Lotfi, S., Maleki, B., Hemmati, S., 2021. Bio-inspired synthesis of palladium nanoparticles fabricated magnetic Fe 3 O 4 nanocomposite over Fritillaria imperialis flower extract as an efficient recyclable catalyst for the reduction of nitroarenes. Sci. Rep. 11, 1–15.
Waris, A., Din, M., Ali, A., Afridi, S., Baset, A., Khan, A.U., Ali, M., 2021. Green fabrication of Co and Co3O4 nanoparticles and their biomedical applications: a review. Open Life Sci. 16, 14–30.
Williams, C.A., 2013. Specialized dietary supplements. Equine Clin. Appl. Nutrit. 351–366.
Zhang, Y., He, S., Guo, W., Hu, Y., Huang, J., Mulcahy, J.R., Wei, W.D., 2017. Surface-plasmon-driven hot electron photochemistry. Chem. Rev. 118, 2927–2954.
Zhao, J., Yang, G., Zhang, Y., Zhang, S., Zhang, C., Gao, C., Zhang, P., 2021. Controllable synthesis of different morphologies of CuO nanostructures for tribological evaluation as water-based lubricant additives. Friction 9, 963–977.
Zhou, Y., Yu, W., Cao, J., Gao, H., 2020. Harnessing carbon monoxide-releasing platforms for cancer therapy. Biomaterials 255, 120193.